

2014

# BioTechnology

*An Indian Journal*

FULL PAPER

BTAIJ, 10(24), 2014 [16291-16298]

## Analysis of garden waste composting and the effects of humic acid content using near-infrared spectroscopy

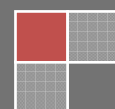
Zhen Liu, Xiang Yang, Anlong Zou, Yaning Luan\*  
College of Forestry, Beijing Forestry University, Beijing 100083, (CHINA)  
Email: luanyaning@bjfu.edu.cn

### ABSTRACT

In this study, we used near-infrared spectroscopy (NIRS) to evaluate the effects of adding humic acid (HA) to garden waste compost and to estimate the optimum HA content. We prepared four treatments with addition of 0, 5, 10, and 15% HA to a garden waste pile and used NIRS to analyze changes after various composting periods. The results of the NIRS analysis indicated that additional HA not only accelerates the composting process in the early stages, but also improves the quality of the resulting compost by increasing compost maturity. Based on these results, addition of 15% HA has the most beneficial effects on the process and the resulting compost product.

### KEYWORDS

Near-infrared spectroscopy; Garden waste; Compost; Humic acid.



## INTRODUCTION

In recent years, there have been increasing garden waste (yard trimmings, crop waste, etc.) produced both in China and abroad, with  $2.09\text{--}3.14 \times 10^4$  t/y in Beijing alone<sup>[1]</sup>. Composting<sup>[2-3]</sup> of garden waste is currently considered to be the most effective and environmentally benign way to achieve waste recycling<sup>[4-5]</sup>, compared with landfill or incinerate. The main components of garden waste are fibrin, hemicellulose, lignin, etc. Of these, fibrin is the most abundant, but is usually combined with the other two and protected by lignin in the cell walls, which makes it difficult to be broken down.

Humic acid (HA), an exogenous natural additive for controlling nitrogen loss in composting, can enhance degradation of fibrin, hemicellulose, and lignin and transform them to stable humic substances<sup>[6-9]</sup>, which reflect the maturity of the compost. However, if too much HA is added, it can cause several harmful effects<sup>[6-9]</sup>.

Infrared (IR) spectra reflect IR absorption of molecular vibrations. Compared with traditional methods for evaluating the maturity of compost, IR spectroscopy requires a small sample, is nondestructive, and has the advantage of being a simple, accurate approach to long-term monitoring of waste composting. In recent years, spectroscopic techniques such as near-IR spectroscopy (NIRS), Fourier transform IR (FT-IR), electron spin resonance (ESR), and nuclear magnetic resonance (NMR) have been used to study changes in organic matter during composting<sup>[10-13]</sup>. However, these changes vary substantially for different materials and conditions, particularly for organic compounds<sup>[14,15]</sup>. To date, there have been few systematic studies of the characteristics of IR spectra of garden waste compost.

Therefore, the objectives of this research were to obtain an overview of the changes in organic materials that take place during composting with different amounts of HA and to determine the characteristics of the IR spectra of these materials. We added 0, 5, 10, and 15% (fresh weight) HA to garden waste and obtained NIRS spectra at different stages of composting. Chemical changes (based on functional groups) were evaluated based on differences in the magnitudes and wavenumbers of the absorption peaks of the NIRS spectra<sup>[16,17]</sup>.

## EXPERIMENTAL SECTION

### Materials

Garden wastes, including litter, branches, and leaves from poplar, willow, white wax, and weed (1:1:1:1) that were mixed and freeze-dried, with a pH of 6.30, an organic carbon mass fraction of 47.61%, and a total nitrogen (TN) mass fraction of 0.79%. The HA had an 18% water content, 0.16% TN, 6.48 pH, and 39.5% organic carbon ( $395.42 \text{ g}\cdot\text{kg}^{-1}$ ).

### Compost methods

Four compost piles were prepared with 0, 5, 10, and 15% HA, each measuring 2 m long, 1.5 m wide, and 1 m high. The compost piles were sampled 0, 6, 15, and 32 d after initiation of composting. Each compost sample was prepared by mixing five subsamples from different locations within the pile.

### NIRS methods

The dried samples were compressed with KBr into tablets and analyzed using a Perkin Elmer Spectrum 100 FT-IR (Shelton, CT, USA) over a scanning wavelength range of  $4000\text{--}450 \text{ cm}^{-1}$  with a spectral resolution of  $4 \text{ cm}^{-1}$ . For each sample, 32 scans were accumulated for each spectrum. We used Origin 9.0 analysis software to process the data.

## RESULTS AND DISCUSSION

### Analysis of the degradation process

The maturity of compost can be assessed by many measures, including degree of seed germination, extractable lipids, optical density and colorimetric tests by  $^{13}\text{C}$  NMR spectroscopy, and

pyrolysis field ionization mass spectrometry<sup>[5,16,18,19]</sup>. Previous studies with these tests have shown that garden waste was composted to a large extent after about 2 wk and was completely mature after 4 wk<sup>[2,5,20]</sup>. Therefore, considering the physical characteristics of the organic wastes, we divided the degradation into the following periods: the heating period and the high-temperature period during 0–6 d, the cooling period during 7–15 d, a slight rebound in temperature after the 15th d, which is known as the second compost stage, and the 32nd d came to maturity. The characteristic peaks of the garden compost sample spectra were attributed as shown in TABLE 1<sup>[11-13,21]</sup>.

**TABLE 1: Attribution of absorption bands in the infrared spectrogram**

Wavenumber (cm <sup>-1</sup> )	Assignment	Source
3417	$\nu(\text{OH}^-)$ , (NH)	Alcohol, phenol, carboxyl (COOH), and N–H (amide) groups
2923	$\nu_{\text{as}}(\text{CH}_2)$	C–H asymmetric, C–H stretch of –CH aliphatic
2853	$\nu_{\text{as}}(\text{CH}_2)$ , $\nu_{\text{as}}(\text{CH}_3)$	C–H asymmetric, C–H stretch of –CH aliphatic
1620	$\nu_{\text{as}}(-\text{COO}^-)$ , $\nu(\text{C}=\text{C})$ , $\delta(\text{N}-\text{H})$ , $\nu(\text{C}=\text{O})$	Aromatic structure, $\text{COO}^-$ and C=O groups (e.g., amides, ketones and quinines)
1509	$\delta(\text{CH}_2, \text{CH}_3)$	Carbohydrates, aliphatic compounds, amino acid salts, aromatic rings of lignins, amide compounds
1427	$\nu(\text{C}-\text{O})$ , $\delta_s(\text{CH}_2)$ , $\nu_{\text{ring}}$ , $\nu_{\text{as}}(-\text{COO}^-)$ , $\delta(\text{OH})$	Several aliphatic structures, phenolic OH groups, $\text{COO}^-$ groups, stretching vibrations of aromatic rings and carbonates
1415	$\nu(\text{C}-\text{O})$ , $\delta_s(\text{CH}_2)$ , $\nu_{\text{ring}}$	Aromatic rings of lignins, aliphatic compounds, organic carboxylic acid salt
1398	$\nu_{\text{as}}(-\text{COO}^-)$	Ammonium carbonate formed by reaction of ammonia and $\text{CO}_2$
1319	$\delta(\text{OH})$	Carbohydrates
1241	$\nu_{\text{as}}(-\text{COO}^-)$ , $\delta(\text{OH})$	Carboxylates
1034	$\nu(\text{C}-\text{O})$ , $\nu_{\text{ring}}$ , $\nu(\text{Si}-\text{O})$	C–O stretch of polysaccharides, Si–O asymmetric stretch of silicate impurities
917	$\delta(-\text{CO}_2^{-3})$ , $\nu(\text{C}-\text{C})$	Aromatic rings and halogens (chloro-compounds)
780	$\nu(\text{Si}-\text{O})$	Aromatic rings and halogens (chloro-compounds) and Si–O asymmetric stretch
670	$\nu_{\text{ring}}$	Aromatic rings and halogens (chloro-compounds)
478	$\nu(\text{OH})$	Phosphate as orthophosphoric acid

### NIRS analysis of the untreated samples

The functional group peak intensities for raw garden waste were determined using the spectrum for the raw material on the 1st day over the wavenumber range from 400 to 4000 cm<sup>-1</sup> (Figure 1). There were clear absorption peaks at 3417 (stretching vibration in O–H), 1620 (lignin conjugate aryl ketone C=O stretching vibration), 1034, and 478 (OH out of plane bending) cm<sup>-1</sup> and weak absorption peaks at 2923 (aliphatic C–H stretching vibration), 1509 (telescopic aromatic C=C), 1427 (aliphatic  $\text{NO}_2$  antisymmetric stretching, and 1231 (the C–O stretching vibration absorption peak of carboxyl in the weak) cm<sup>-1</sup>. Based on TABLE 1, the raw garden waste had absorption bands attributed to stretching of aromatic C=C at 1509 cm<sup>-1</sup>; the double bond or carbonyl group attached to the –CH<sub>2</sub> deformation vibration of lignin and vibration of inorganic  $\text{NH}_4^+$ ,  $\text{NO}_3^-$ , and organic carboxylic acid salt at 1419–1427 cm<sup>-1</sup>; and C–H and C–O absorption bands at 1319 cm<sup>-1</sup>. In addition, the polysaccharide compound bands at 950–1170 cm<sup>-1</sup> are generally attributed to the starchy fibers of plant materials in organic waste. The Si–O–Si asymmetric stretching vibration band can be seen around 1034 cm<sup>-1</sup>. And 670 cm<sup>-1</sup> is also the characteristic peak of aromatic ring type<sup>[10,21,22]</sup>.

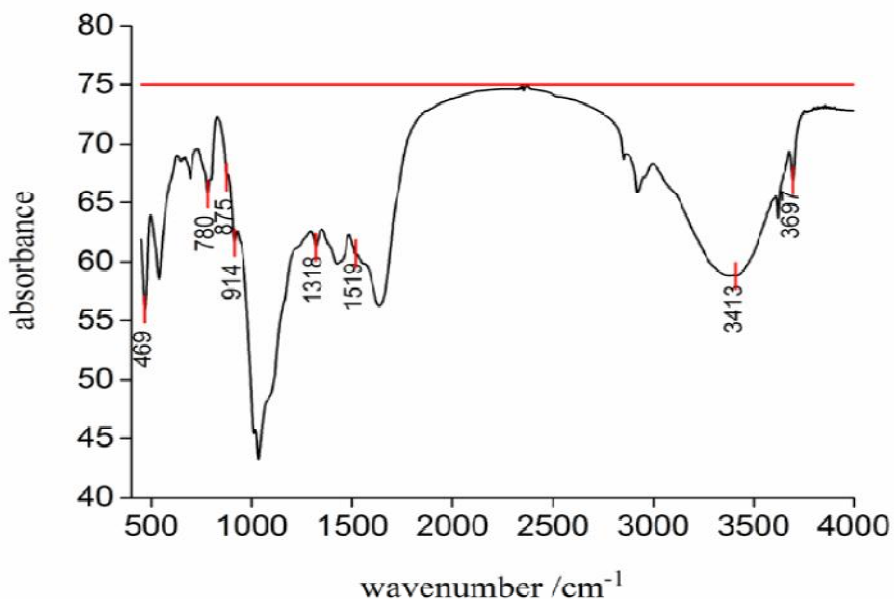


Figure 1: FT-IR spectra of raw materials before composting

The characteristic absorption bands described above indicate the presence of abundant carbohydrates (lignin, cellulose, hemicellulose, etc.) and some proteins, amide compounds, and silicate minerals. However, the lack of absorbance during 2200–2400  $\text{cm}^{-1}$ , which includes multiple complex bands for  $\text{NH}_4^+$ , indicates that the garden waste was low in proteins.

#### NIRS analysis of the samples treated with humic acid

During the composting process, the characteristic peaks gradually changed in intensity until they reached a stable state. As the Figure 2 shows, in the heating period and the high-temperature period (0–6 days), near the 3400  $\text{cm}^{-1}$ , –OH and N–H peak decreased significantly, while lignin related band, 1650–1630  $\text{cm}^{-1}$ , there was a relatively small decrease. Vibration of aromatic amines at 1320  $\text{cm}^{-1}$  gradually decreased and eventually nearly disappeared on the 32nd day, reflecting the effects of glycolysis in maturing compost, which made other more stable functional groups with simple structures be formed. A small peak appeared at 1720–1740  $\text{cm}^{-1}$  and quickly disappeared on the 6th day, potentially corresponding to a small amount of volatile compounds.

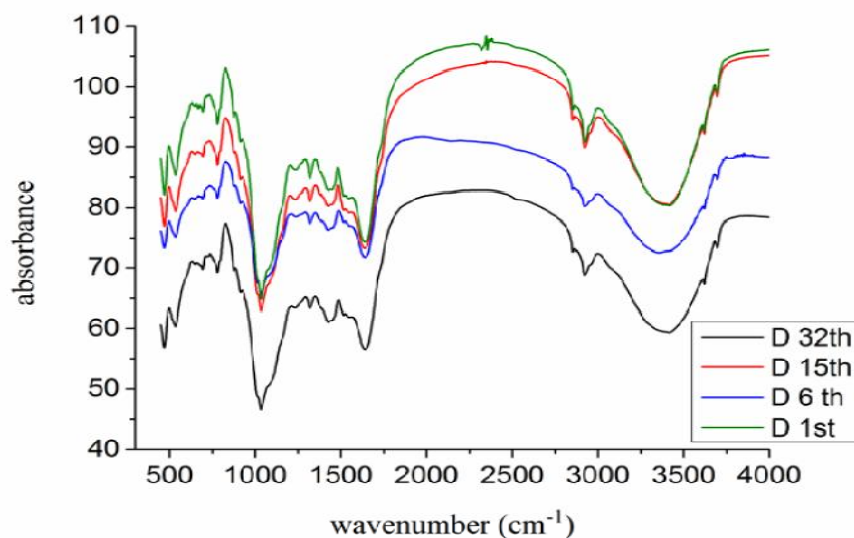


Figure 2: FT-IR spectra of raw materials during degradation

In the cooling-temperature period (7–15 days), from Figure 3 to Figure 4, differences in the characteristic peaks among treatments were less obvious. Compared with the 1st d, the 3400 (–OH, N–H peak) and 2920  $\text{cm}^{-1}$  (C–H stretching vibration peak) areas showed slight weakening. In addition, the lignin- and cellulose-related bands at 1419, 1630, 1325, and 1030  $\text{cm}^{-1}$  decreased, indicating a fair amount of decomposition.

In the second composting stage, from Figure 4 to Figure 5, differences in the characteristic peak intensities became stronger. A sufficiently high temperature allows this second stage of composting and promotes rapid propagation of microorganisms. At 1034, 1419 and 1630  $\text{cm}^{-1}$ , the absorption strength continued to decrease, associated with the aromatic ring skeleton vibration peak and continuous conversion of lipids to carboxylic acid salts and accumulation of HA. At the end of the composting (32nd day), the characteristic peaks are more flattening, aromatic rings stretching vibration peak in 665 and 671  $\text{cm}^{-1}$  significantly increased, proving that the composting process of protein, carbohydrate, fatty compounds is on the decline. Enhancement of aromatization level reflects the curing reaction during decomposition.

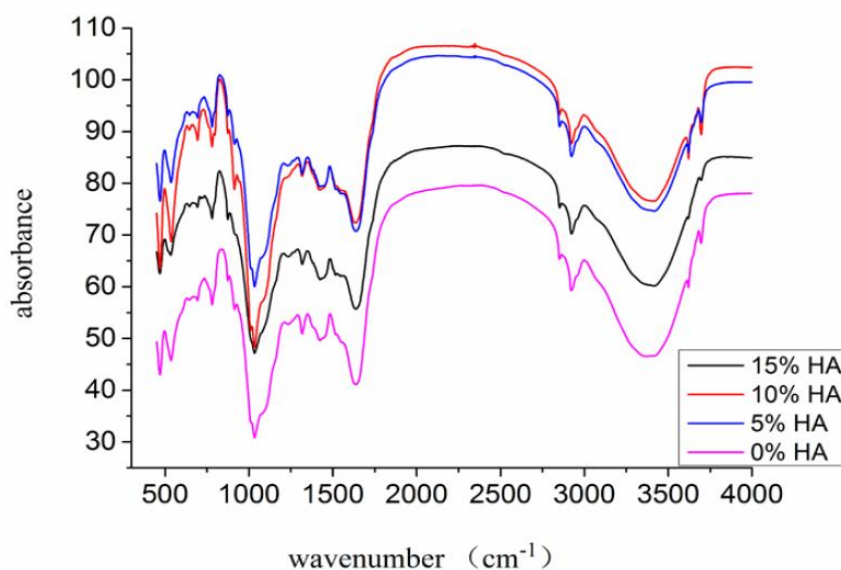


Figure 3: FT-IR spectra of 4 compost piles with HA on the 7th

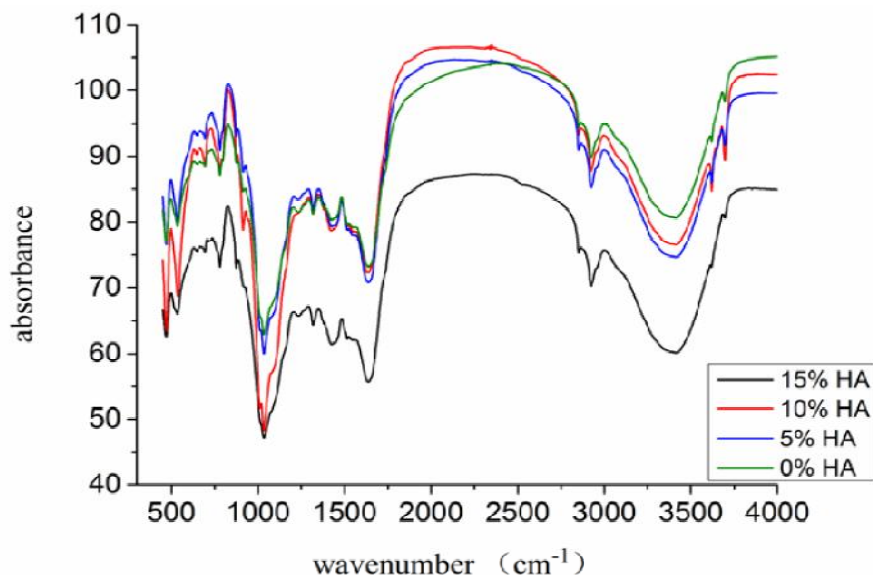


Figure 4: FT-IR spectra of 4 compost piles with HA on the 15th

Samples with different humic acid contents contained similar functional groups, as demonstrated by their NIRS spectra with basically consistent absorption peaks. However, the intensities of the characteristic peaks of the functional groups differed. Near  $3400\text{ cm}^{-1}$ , the  $-\text{OH}$  and  $\text{N}-\text{H}$  peak decreased significantly, while the change in the absorption intensity of the lignin-related bands at  $1630$  and  $1325\text{ cm}^{-1}$  was relatively small (Figure 3). Therefore, at this stage, proteins and carbohydrates are relatively easy to decompose into simpler substances. A small increase in the absorption intensity at  $2920$  and near  $1419\text{ cm}^{-1}$  was evidence of oxidative degradation reactions<sup>[11]</sup>, cracking of large aliphatic hydrocarbon molecules into short chain hydrocarbons and small molecules, with  $-\text{CH}_2$  groups and carboxyl groups increasing in number.

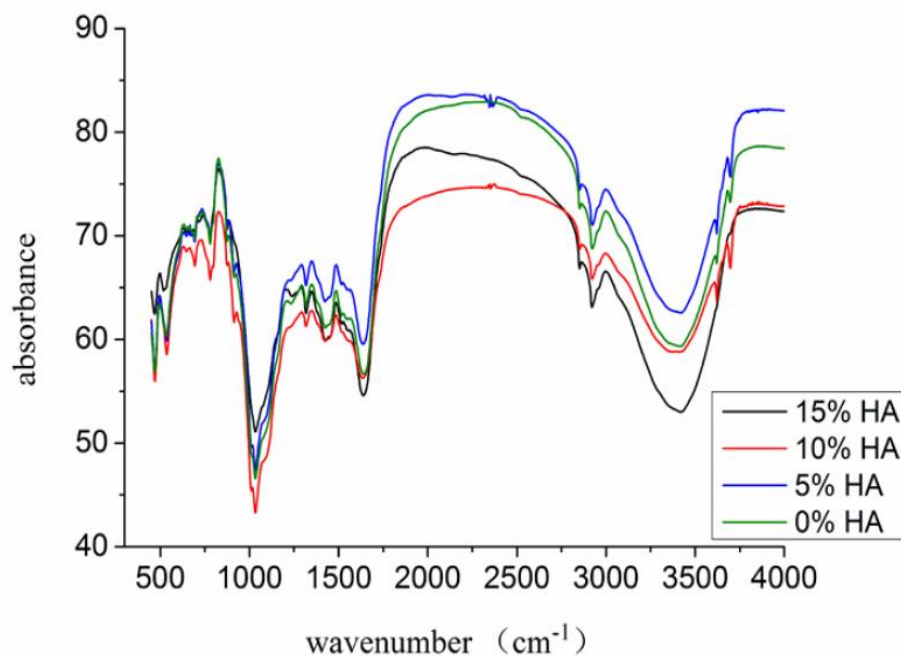


Figure 5: FT-IR spectra of 4 compost piles with HA on the 32nd

Comparing Figure 3 with Figure 2, treatment with different amounts of HA not only didn't change the material results of the composting process or the decomposition order. What's more, increased HA was associated with decreases near  $1300\text{ cm}^{-1}$  in the carbohydrate group characteristic peak strength, which had nearly disappeared on the 32nd d. Therefore, increasing the addition of HA can significantly accelerate the decomposition rate of the compost. At the same time, the characteristic absorption peak for  $\text{N}-\text{H}$  at  $3400\text{ cm}^{-1}$  decreased gradually, indicating decomposition of protein amide compounds to simple salts, increasing the nitrogen content of the compost. In Figure 4, compared with 5 and 10% HA groups, the addition of 15% HA group had the most obvious result, possibly because HA inhibits microbial activity to a certain degree, reducing nitrogen losses. In Figure 5 the main stretching vibration absorption peak reached a maximum, because the aliphatic component (polysaccharide fatty amide) had decomposed and aromatic structures, organic acid salts, and inorganic salts had increased greatly. Therefore, addition of HA improved the compost quality. During the composting process, multimerization of organic unsaturated structures occurred, increasing the aromatic content. Alkyl, amino, and polysaccharide peaks flattened out, because as the HA level increased, functional group structures became simpler. We can conclude that 15% HA can speed up decomposition of proteins, small molecular substances such as carbon sources, and raise the degree of compost Fong and significantly speed up the composting process. Similar results have been reported for finished compost for polysaccharides, lipids, and amide content, and it has been demonstrated that too high HA content causes undesirable effects<sup>[14,16]</sup>. Therefore, 15% HA content is considered to be the most appropriate.

## CONCLUSIONS

During composting of the garden waste, small molecules, cellulose, hemicellulose, lignin, and other organic macromolecules were degraded, resulting in a higher degree of condensation and simpler but more stable humus. Moreover, the addition of HA increased the rate of this process without changing the degradation mechanisms or decomposition products. HA also improved the quality of the compost by more completely degrading the organic compounds. In the experiment, microbial first breaking down carbohydrates, protein and some easy to decompose the organic matter, only if can decompose substances of microbial growth, reproduction is insufficient to meet demand, microbes will break down some of the refractory material. In this study, 15% HA content was found to be most effective.

## ACKNOWLEDGMENTS

This study was supported by the Fundamental Research Funds for the Central Universities (NO. YX2013-09).

## REFERENCES AND NOTES

- [1] N.Zhang, I.D.Williams, S.Kemp, N.F.Smith; Greening academia: Developing sustainable waste management at higher education institutions, *Waste Management*, **31**, 1606-1616 (2011).
- [2] O.S.Adebayo, N.A.Kabbashi, M.Z.Alam, A.Saliu, A.Abass, T.I.D.Ruqayyah; Composting of food and yard wastes by locally isolated fungal strains, *African Journal of Biotechnology*, **10**, 18800-18806 (2011).
- [3] R.Van Haaren, N.J.Themelis, M.Barlaz; Lca comparison of windrow composting of yard wastes with use as alternative daily cover (adc), *Waste Management*, **30**, 2649-2656 (2010).
- [4] N.W.Zhu, C.Y.Deng, Y.Z.Xiong, H.Y.Qian; Performance characteristics of three aeration systems in the swine manure composting, *Bioresource Technology*, **95**, 319-326 (2004).
- [5] A.Nadeem, S.Baig, K.Iqbal, N.Sheikh; Impact of laccase enzyme inducers on solid waste compost maturity and stability, *Environmental Technology*, **35**, 3130-3138 (2014).
- [6] N.Q.Arancon, C.A.Edwards, S.Lee, R.Byrne; Effects of humic acids from vermicomposts on plant growth, *European Journal of Soil Biology*, **42**, S65-S69 (2006).
- [7] N.Q.Arancon, S.Lee, C.A.Edwards, R.Atiyeh; Effects of humic acids derived from cattle, food and paper-waste vermicomposts on growth of greenhouse plants, *Pedobiologia*, **47**, 741-744 (2003).
- [8] I.Azcona, I.Pascual, J.Aguirreolea, M.Fuentes, J.Maria Garcia-Mina, M.Sanchez-Diaz; Growth and development of pepper are affected by humic substances derived from composted sludge, *Journal of Plant Nutrition and Soil Science*, **174**, 916-924 (2011).
- [9] A.Traversa, E.Loffredo, C.E.Gattullo, A.J.Palazzo, T.L.Bashore, N.Senesi; Comparative evaluation of compost humic acids and their effects on the germination of switchgrass (*panicum vigatum* l.), *Journal of Soils and Sediments*, **14**, 432-440 (2014).
- [10] A.Jouraihy, S.Amir, M.El Gharous, J.C.Revel, M.Hafidi; Chemical and spectroscopic analysis of organic matter transformation during composting of sewage sludge and green plant waste, *International Biodeterioration & Biodegradation*, **56**, 101-108 (2005).
- [11] B.Lv, M.Xing, J.Yang, W.Qi, Y.Lu; Chemical and spectroscopic characterization of water extractable organic matter during vermicomposting of cattle dung, *Bioresource Technology*, **132**, 320-326 (2013).
- [12] M.R.Provenzano, A.D.Malerba, D.Pezzolla, G.Gigliotti; Chemical and spectroscopic characterization of organic matter during the anaerobic digestion and successive composting of pig slurry, *Waste Management*, **34**, 653-660 (2014).
- [13] L.T.Shirshova, E.A.Ghabbour, G.Davies; Spectroscopic characterization of humic acid fractions isolated from soil using different extraction procedures, *Geoderma*, **133**, 204-216 (2006).
- [14] V.D'Orazio, N.Senesi; Spectroscopic properties of humic acids isolated from the rhizosphere and bulk soil compartments and fractionated by size-exclusion chromatography, *Soil Biology & Biochemistry*, **41**, 1775-1781(2009).
- [15] Z.Droussi, V.D'Orazio, M.Hafidi, A.Ouatmane; Elemental and spectroscopic characterization of humic-acid-like compounds during composting of olive mill by-products, *Journal of Hazardous Materials*, **163**, 1289-1297 (2009).

- [16] D.S.Kumar, P.S.Kumar, N.M.Rajendran, G.Anbuganapathi; Compost maturity assessment using physicochemical, solid-state spectroscopy, and plant bioassay analysis, *Journal of Agricultural and Food Chemistry*, **61**, 11326-11331 (2013).
- [17] V.Miikki, K.Hanninen, J.Knuutinen, J.Hyotylainen, R.Alen; Characterization of the humic material formed by composting of domestic and industrial biowastes, Part 1, Hplc of the cupric oxide oxidation products from humic acids, *Chemosphere*, **29**, 2609-2618 (1994).
- [18] D.Raj, R.S.Antil; Evaluation of maturity and stability parameters of composts prepared from agro-industrial wastes, *Bioresource Technology*, **102**, 2868-2873 (2012).
- [19] D.Raj, R.S.Antil; Evaluation of maturity and stability parameters of composts prepared from farm wastes, *Archives of Agronomy and Soil Science*, **58**, 817-832 (2012).
- [20] F.Barje, L.El Fels, H.El Hajjouji, P.Winterton, M.Hafidi; Biodegradation of organic compounds during co-composting of olive oil mill waste and municipal solid waste with added rock phosphate, *Environmental Technology*, **34**, 2965-2975 (2013).
- [21] S.A.Mireei, M.Sadeghi; Detecting bunch withering disorder in date fruit by near infrared spectroscopy, *Journal of Food Engineering*, **114**, 397-403 (2013).
- [22] M.S.Kumar, P.Rajiv, S.Rajeshwari, R.Venckatesh; Spectroscopic analysis of vermicompost for determination of nutritional quality, *Spectrochimica Acta Part a-Molecular and Biomolecular Spectroscopy*, **135**, 252-255 (2015).